

Cyclic changes in keratocyte speed and traction stress arise from Ca^{2+} -dependent regulation of cell adhesiveness

Andrew D. Doyle and Juliet Lee*

Department of Molecular and Cell Biology, University of Connecticut, Storrs, CT 06269, USA

*Author for correspondence (e-mail: jlee@uconnvm.uconn.edu)

Accepted 12 October 2004
Journal of Cell Science 118, 369-379 Published by The Company of Biologists 2005
doi:10.1242/jcs.01590

Summary

The activation of stretch-activated calcium channels (SACs) in keratocytes can induce spatially coordinated increases in traction stress that promote protrusion at the cell front, while simultaneously inducing retraction at the rear. To investigate how this occurs, we correlated calcium-induced changes in traction stress with alterations in cell speed and shape. Cyclic changes in these parameters were associated with each calcium transient. In addition, an inverse relationship was found between traction stress and cell speed, suggesting that alternating changes in adhesiveness were occurring at the rear. We investigated this further by inhibiting or inducing calcium transients and observing the effects on traction stress, cell speed and shape. Inhibition of calcium transients prevented

retraction and led to a slow increase in traction stress. In addition, large aggregates of vinculin developed at the lateral rear edges of treated keratocytes, consistent with an increase in adhesiveness. Induction of a calcium transient resulted in a rapid retraction, involving both increased traction stress and adhesion disassembly at the rear. We also found that keratocytes exhibiting frequent transients generated larger traction stress and moved significantly faster than other cells. Together, these data suggest that calcium transients coordinate changes in adhesiveness with SAC-mediated cycles of mechano-chemical feedback.

Key words: Keratocyte, Regulation, Motility, Adhesion, Force, Calcium

Introduction

Cell movement requires the coordination of several different cytoskeletal functions so that continuous cycles of protrusion and retraction can occur (Mitchison and Cramer, 1996; Pollard and Borisy, 2003). This involves maintaining a net increase in actin polymerization and adhesion formation at the front edge, while cell detachment and retraction occurs at the rear. Although much has been learnt about the molecular mechanisms underlying these processes, it is not known how they are coordinated, yet this is a fundamental determinant of cell speed and mode of movement. For example, slow-moving cell types such as fibroblasts exhibit a discontinuous mode of movement in which protrusion and retraction occur in two temporally distinct phases (Chen, 1979). By contrast, these phases can occur simultaneously in fish epithelial keratocytes, resulting in a rapid, highly efficient mode of movement (Lee et al., 1993). There is considerable evidence that the generation of mechanical force is involved in coordinating cytoskeletal functions (Lauffenberger and Horwitz, 1996); therefore, learning how this is achieved is central to understanding how molecular processes are integrated to produce cell movement.

Early studies of fibroblasts were some of the first to recognize the importance of cytoskeletal tension in coordinated cell movement. The retraction-induced spreading (RIS) model was based on the observation that a surge in protrusion rate follows retraction at the rear (Chen, 1981). The proposal that increasing cytoskeletal tension inhibits protrusion but

facilitates retraction was supported by the finding that the rates of these processes are inversely proportional to each other (Chen, 1979). Thus, cyclic changes in cytoskeletal tension could allow alternate phases of protrusion and retraction to occur. Other studies have also shown that cytoskeletal tension inhibits protrusion (Kolega, 1986; Lee et al., 1993) but favors retraction (Chen, 1981; Lee et al., 1994; Crowley and Horwitz, 1995). The converse has also been found to be true (Leader et al., 1983; Oliver et al., 1999). The spatial distribution of cytoskeletal tension, as inferred from the use of traction force assays and observations of cytoskeletal organization, has a major influence on the mode of cell movement. In cells that display discontinuous movement, the largest contractile forces are oriented inward between the front and rear of the cell, and parallel to the direction of movement (Harris, 1980; Galbraith and Sheetz, 1997; Oliver et al., 1999; Pelham and Wang, 1999). However, in keratocytes, the largest contractile forces are oriented inward between the left and right lateral cell edges, and perpendicular to the direction of movement (Lee et al., 1994; Burton et al., 1999; Oliver et al., 1999).

Cytoskeletal tension arises from the generation of inward directed contractile forces that are opposed by cell adhesions located primarily at the cell edge. Therefore, changes in adhesiveness or contractility will alter the degree of cytoskeletal tension and thus the likelihood of protrusion or retraction. Furthermore, the local regulation of adhesion strength and contractility is required for continuous cell

movement. For example, in well-polarized, motile fibroblasts the adhesion-cytoskeletal linkage was found to be stronger at the front than at the rear of the cell (Schmidt et al., 1993); when an asymmetry in adhesion strength does not occur, cell polarity and speed are significantly reduced. The highly coordinated movement of fish keratocytes has been attributed to variations in the local ratio of adhesiveness to contractility along the cell margin (Lee et al., 1994). According to this idea, a high rate of protrusion is favored at the front of the cell where contractility is low and the area of adhesive contact is large. At the cell rear, retraction occurs because contractile forces exceed cell adhesion strength thus causing cell detachment.

Intracellular calcium regulates many of the molecular processes that are essential for cell movement, including cytoskeletal dynamics, contractility and adhesion turnover (Stossel, 1993; Sjaastad and Nelson, 1996). Calcium imaging experiments have shown that increases in $[Ca^{2+}]_i$ can specify the location and timing of retraction. For instance, a gradient of $[Ca^{2+}]_i$ has been found to increase towards the rear of some highly motile cell types (Brundage et al., 1991; Gilbert et al., 1994; Brust-Mascher and Webb, 1998). This is believed to localize calcium-dependent cell detachment mechanisms such as increased contractility (Walker et al., 1998; Eddy et al., 2000; Zeng et al., 2000), enzymatic adhesion disassembly (Hendey et al., 1992; Huttenlocher et al., 1997; Giannone et al., 2002) or increased actin severing (Hartwig and Yin, 1988) to the rear. The role of calcium in triggering retraction is particularly evident in cells that display transient increases in $[Ca^{2+}]_i$ (Marks and Maxfield, 1990; Mandeville et al., 1995; Nebl and Fisher, 1997; Lee et al., 1999). In these cells, calcium transients are often observed immediately before a retraction. However, when calcium transients are inhibited, retraction fails to occur and cell movement is halted (Marks and Maxfield, 1990; Lee et al., 1999). Furthermore, local increases in $[Ca^{2+}]_i$ that occur within the filopodia of nerve growth cones induce retraction in this region, while promoting outgrowth on the opposite side (Gomez et al., 2001). The calcium-activated protein calpain has been shown to orchestrate the necessary changes in adhesiveness for this response (Robles et al., 2003).

In fish keratocytes, calcium transients are triggered by the activation of stretch-activated calcium channels (SACs), and this is believed to occur in response to increasing cytoskeletal tension, when retraction and, consequently, cell movement is impeded (Lee et al., 1999). The calcium-induced retraction then reduces cytoskeletal tension, allowing cell movement to resume. Thus, SACs provide a mechano-chemical feedback mechanism that promotes a rapid, continuous mode of movement. Recently, we measured the changes in traction force production, an indicator of cytoskeletal tension, associated with single calcium transients (Doyle et al., 2004). We found that calcium transients lead to increased traction stress production that is sustained until retraction occurs. These temporal changes in traction stress were also accompanied by a sequence of changes in their spatial distribution, which together suggested their role in maintaining a rapid, continuous mode of movement.

To investigate how SAC-induced calcium transients regulate the generation of traction force in relation to cell movement, we have correlated calcium-induced changes in traction stress with measures of cell speed and shape during one cycle of

mechano-chemical feedback. In addition, we examined changes in these parameters when different phases of the feedback cycle were either promoted or inhibited. Our findings reveal a mechanism by which the regulation of cell adhesiveness is integrated into the mechano-chemical feedback regulation of cell movement.

Materials and Methods

Reagents

A 1 mM stock solution of gadolinium hydrochloride III (Gd^{3+}) (Sigma-Aldrich Co., St Louis, MO) was diluted in Fish Ringer's solution containing Mg^{2+} (0.49 mM) and Ca^{2+} (0.90 mM). Gd^{3+} was used at a working concentration of 100 μ M diluted in Fish Ringer's solution, containing a low concentration of fetal calf serum (~2%). Stock solutions of EGTA and EDTA (Sigma-Aldrich Co.) at 200 mM were made in PBS and pH-balanced to 7.25. This was added directly to culture dishes to obtain a final working concentration of 10 mM for EGTA and 5 mM for EDTA. A stock solution of calcimycin (A-23187, free acid) (Molecular Probes) was made up to 50 mM in DMSO. Before use, this was diluted in Fish Ringer's with 2% serum to a working concentration of 5 μ M.

Preparation and calibration of the gelatin substrata

Gelatin substrata were prepared as described previously (Doyle and Lee, 2002). Briefly, 400 μ l of a solution containing 3.0% gelatin (Nabisco, Parsippany, NJ) dissolved in Ca^{2+} and Mg^{2+} free Fish Ringer's was transferred into a Rapport chamber and allowed to solidify at 4°C. A solution containing either flash red microspheres (0.2 μ m) (Bangs Laboratories, Fishers, IN) or blue fluorescent fluospheres (Molecular Probes) was added to the gelatin substratum and the excess aspirated off immediately. The remaining bead solution was allowed to dry on to the gelatin substratum for one hour at 4°C under airflow. Gelatin substrata were then briefly (5-15 seconds) warmed on a hot plate to liquefy the lower layer of gelatin. After removal from the hot plate ~330 μ l of the gelatin solution was carefully aspirated from the bottom of the chamber using a small pipette tip. Gels were then rapidly cooled for 30 seconds by placing cell chambers on a level metal sheet, pre-cooled to -20°C.

Calibrations of the substrata were performed by placing a steel ball (diameter=0.3-0.4 mm, density=14.95 g/cm³) (Hoover Precision, East Granby, CT) on the substratum and measuring the resulting surface indentation (Lo et al., 2000).

Measurement of substrate displacement

For each period of observation a series of one image of beads in their disturbed or displaced positions was obtained and another reference image of beads in their undisplaced positions, after the cell had moved away. Displacement of the substratum was calculated by comparing the positions of marker beads between the disturbed and reference image, using a correlation based optical flow algorithm (Marganski et al., 2003).

Generation of traction maps

Using the traced cell outline as a guide, a custom algorithm was then used to generate a mesh of approximately 200 quadrilateral elements tessellating the interior of the cell. The most probable traction vector at each node of this mesh was then estimated by fitting the displacement data using the formulae of Boussinesque relating substrate displacement to delta function forces acting at the substrate surface. Because a cell cannot apply a net force or torque on the substrate the fitting routine also included elements that enforce these necessary constraints (for details, see Dembo and Wang, 1999).

Preparation of cells for calcium imaging

Fish epithelial keratocytes were cultured from Molly fish *Poecilia sphenops* scales as described previously (Lee et al., 1993; Doyle and Lee, 2002). Keratocytes were loaded with the calcium indicator Calcium Green™-1 dextran (3000 M_r) (Molecular Probes, Eugene, OR) using the Influx™ pinocytotic cell-loading reagent (Molecular Probes), which was modified for use with keratocytes (Doyle and Lee, 2002). Keratocytes were then replated onto gelatin substrata.

Calcium imaging

Calcium imaging was performed as described previously, (Ishihara et al., 1997). Before imaging, culture medium was replaced with L-15 medium with low serum (~2%), without antibiotics or antifungal agents, to reduce background fluorescence. Calcium imaging was performed on an inverted microscope (Eclipse TE 300) (Nikon, Melville, NY) using a Plan APO 100×/1.4 oil emersion objective (Nikon). Fluorescence excitation was achieved using a Ludl high-speed dual filter wheel (Ludl electronic production Ltd, Hawthorne, NY) fitted with HQ500/20 and D560/40 excitation filters (Chroma Technology Corp., Brattleboro, VT) for visualization of Calcium Green-1 dextran and the marker beads, respectively. Emitted fluorescence was collected using a DAPI/FITC/Texas Red triple band pass filter set (Chroma Technology Corp.). Images were acquired using a back-illuminated, frame transfer CCD camera (Quantix 57) (Roper Scientific, Tucson, AZ). Isee Analytical Imaging Software (Isee Imaging Systems, Raleigh, NC) running on a Unix platform (SGI O²) (Silicon Graphics, Mountain View, CA) was used for image acquisition and hardware control. Paired images of Calcium Green-1 fluorescence in moving keratocytes and marker beads were collected approximately every 1.8 seconds for several minutes and stored on the computer hard drive. Triple imaging of some cells was performed using a Zeiss 100×/1.4 emersion oil objective on a Zeiss Axiovert 200 M inverted microscope (Carl Zeiss MicroImaging, Thornwood, NY) equipped with a DG-4 filter-changer (Sutter Instruments Co., Novato, CA). Three images of the calcium indicator fluorescence, calcium insensitive rhodamine dextran, both co-loaded into keratocytes, and marker beads were acquired using FITC, Texas Red and Cy-5/DAPI excitation filters, respectively, every ~1.8 seconds. Emitted fluorescence was collected using a DAPI/FITC/Texas Red/Cy-5 quad band pass filter set (Chroma Technology Corp.) An Orca II CCD camera (Hamamatsu Corp., Bridgewater, NJ) controlled by Openlab software (Improvision) on an Apple G4 platform was used for image acquisition. To detect changes in $[Ca^{2+}]_i$, measurements of the average fluorescence intensity were made over the cell body region in sequential, background subtracted images.

Procedure for imaging treated keratocytes

Owing to the inherent variation in traction stress production, cell speed and shape it was necessary to acquire a sequence of images over a 1-3 minute period, before treatment. This facilitated the identification of changes in cell behavior due to the effect of the treatment from the normal untreated state. Solutions containing Gd^{3+} , Ca^{2+} -free medium or calcimycin were added via pipette, while simultaneously withdrawing culture medium using a micropipette attached to a micromanipulator (Harvard Apparatus, Holliston, MA). Solutions containing EGTA or EDTA were added directly to the culture medium and gently mixed.

Interference reflection microscopy

To observe changes in the dynamics and types of adhesions formed, the cell-substratum separation distance was imaged using interference reflection microscopy (IRM). This was performed on a Leica DM IRB inverted microscope (Leica, Germany) using a HCX FLUOTAR 100×/0.60-1.30 oil emersion objective. Images were obtained every

3-5 seconds using a CoolSnap HQ digital camera (Photometrics, Roper Scientific, Tucson, AZ) controlled by Isee Analytical Imaging Software (Isee Imaging Systems, Raleigh, NC) on a linux platform.

Immunofluorescence

Unless otherwise indicated, all steps were performed at 4°C. Before fixation and permeabilization, cells were cooled to 4°C in Fish Ringer's solution. Keratocytes were fixed using two solutions: (1) 2.5% glutaraldehyde (EMS) and 1:200 fluorescein phalloidin (Molecular Probes) in PBS for 40 seconds followed by (2) 1.0% glutaraldehyde and 1:200 fluorescein phalloidin in PBS for 1 minute. Cells were washed two to three times with PBS between each of the following steps: permeabilization in PBS containing 0.25% Triton X-100 and 1:200 fluorescein phalloidin for 4 minutes; incubation in 8°C 1.5% NaBH₄ in PBS for 30 seconds, to reduce auto-fluorescence; blocking with 1.0% BSA for 15 minutes; labeling with anti-vinculin (mouse) antibody (Sigma) (1:100) in PBS for 30 minutes; and labeling with Alexa fluor 568 anti-mouse (Molecular Probes) (1:200) secondary antibody in PBS for 30 minutes. Coverslips were mounted using Antifade light (Molecular Probes). To label EGTA treated keratocytes, cells were incubated in pre-cooled Fish Ringer's containing 10 mM EGTA for 10 minutes followed immediately by fixation.

Morphometric and data analysis

Morphometric analyses were performed using Metamorph analysis software (Universal Imaging). Cell speed was calculated using the x, y coordinates of the cell centroid. The distance between every eleventh centroid was calculated (approx. every 20 seconds), from which a running average of 5 was obtained. Cell shape was measured for each frame, in terms of a shape factor according to the following equation: Shape factor = $(A \times \pi^2)/P$, where A=cell area and P=cell perimeter.

In Fig. 2B, the average percent change in measures of traction stress, speed and shape during the pre-transient phase were calculated by dividing the value of each measure at the initiation of a calcium transient, by the corresponding value ~30 seconds before this. An average of each value was obtained after conversion to a percentage. The average percent change in transduction phase values were obtained as described above after obtaining the relative change in each measure. This was obtained by dividing the maximum (for traction stress) or the minimum (for speed and shape) values of each measure by the initial value at the beginning of the transient. The average percent change in post-transient phase values were calculated as described above. The relative changes in each measure were obtained by dividing the maximum (or minimum) values in the transduction phase by the corresponding minimum (for traction stress) or maximum (for speed and shape) in the post-transient phase.

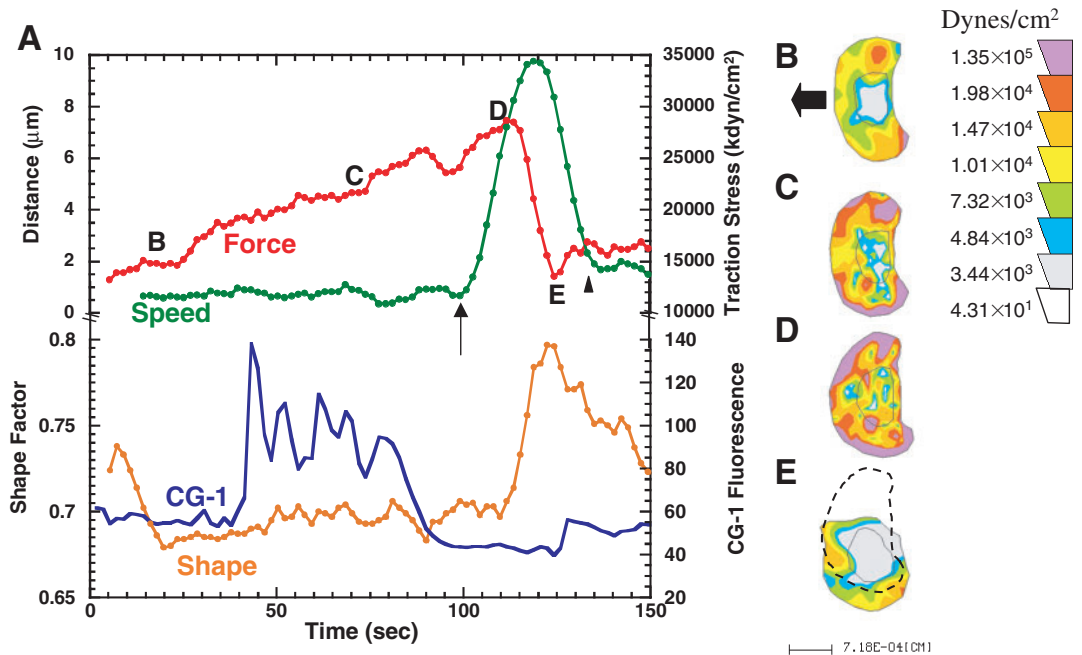
In Fig. 7A the average percent change in traction stress and speed were obtained as described for Fig. 2B. However, the initial ('pre') value for each measure was obtained from a ten-frame average just before a transient, or treatment. The 'peak' value was taken at the maximum (or minimum) point of change, which could be positive or negative. In Fig. 7B rate of change was calculated by dividing the percent change in a measure by time (seconds).

Results

Cyclic changes in traction stress, cell speed and shape are associated with single calcium transients

The activation of SACs is believed to occur in response to increasing cytoskeletal tension that develops when retraction at the rear decreases relative to the rate of protrusion (Lee et al., 1999). The observation of an increased frequency of transients

Fig. 1. Cyclic changes in traction stress, cell speed and shape that accompany a single calcium transient. (A) Plots of the absolute change in 90th percentile traction stress (red), cell speed (green) and shape factor (orange) and $[Ca^{2+}]_i$ as shown by calcium green-1 dextran fluorescence (CG-1; blue). (B-E) Contour maps of traction stress magnitude at corresponding time points marked in A. Shape factor decreases slightly, indicating cell elongation, 38 seconds before the calcium transient. Traction stress begins to increase ~15 seconds before the transient (B) and continues to increase, reaching a maximum ~70 seconds after the onset of the transient (D). Note the region of increased traction stress that enlarges along the cell margin in B-D. During this time period cell movement is completely inhibited. Retraction starts ~60 seconds (arrow) after the calcium transient starts, as shown by the increase in cell speed and the precipitous drop in traction stress (D-E), together with an increase in shape factor, or cell roundness, that occurs ~10 seconds later. When retraction is complete (arrowhead) cell speed returns close to the pre-transient value and cell shape begins to elongate, marking the end of one cycle of mechano-chemical feedback.



in cells with a stretched, fibroblastic morphology is consistent with the idea that more elongated cells experience greater cytoskeletal tension. This is also supported by the finding that elongated fibroblast-shaped keratocytes generate larger traction forces than fan-shaped ones (Oliver et al., 1999). If cell length is proportional to cytoskeletal tension, then elongated keratocytes are expected to move more slowly because of the inhibitory effects that tension has on protrusion. However, the relationship between cytoskeletal tension, cell speed and cell elongation has not been quantified, yet this is important for understanding how force production is related to cell movement.

To investigate how traction stress cell speed and shape are interrelated, we have measured changes in the relative magnitude of these parameters during one cycle of mechano-chemical feedback. In this series of experiments, dual traction force and calcium imaging were performed at high temporal resolution (1 frame every 2 seconds) for several minutes, as described previously (Doyle et al., 2004). For the following analysis we chose cells that displayed distinct calcium transients at intervals greater than ~30 seconds. Plots of 90th percentile traction stress, cell speed and shape showed cyclic changes in these parameters that were associated with a single calcium transient (Fig. 1). To facilitate comparison of these changes, we divided the feedback cycle into three phases (Fig. 2A). The pre-transient phase is defined as the period 30 seconds before the onset of a calcium transient. The transduction phase is taken from the onset of a calcium transient to the start of retraction. This is recognized as the point at which traction stress begins to decrease, that is associated with an increase in speed and cell rounding. The retraction phase is defined as occurring immediately from this point, until changes in traction stress and cell speed are

minimal. The most striking feature of these data is the inverse relationship between cell speed and traction stress during each phase of the feedback cycle (Fig. 2B). On average, a small increase in traction stress occurred together with a small decrease in cell speed before a calcium transient. These changes continued, becoming significant during the transduction phase. On retraction, the relationship between traction stress and cell speed inverted such that the rapid drop in traction stress was accompanied by a significant increase in cell speed (Fig. 2B). Contrary to our expectations, only a small increase in cell elongation was observed during the pre-transient and transduction phases. However, a significant increase in cell rounding did occur during retraction, in accordance with previous observations (Lee et al., 1999; Doyle et al., 2004). It is noteworthy that calcium transients occurred before any significant changes in traction stress, cell speed or shape. This suggests that SACs can respond to either a very small, or highly localized stretch stimulus without global stretching of the cytoskeleton, as previously thought. In relation to this, cross-correlation analysis of area extended versus area retracted showed a high degree of coordination between these events, regardless of cell speed (data not shown). We infer from this that inhibition of retraction will cause an immediate reduction in the rate of protrusion with negligible change in cell shape.

Inhibition of calcium transients prevents adhesion disassembly

It is unclear why retraction and cell movement are impeded when calcium transients are inhibited. It is possible that failure to retract is due to insufficient contractile force generation or lack of adhesion disassembly. To investigate how calcium-

induced changes in traction stress lead to retraction, we have used EGTA, gadolinium (Gd^{3+}) – a SAC blocker – and calcium-free medium to inhibit calcium transients and observed the associated changes in cell speed and shape.

In this first series of experiments, keratocytes were treated with 10 mM EGTA, which chelates extracellular calcium and has been shown to inhibit retraction at the rear in keratocytes and other cell types (Marks and Maxfield, 1990; Lee et al., 1999). On addition of EGTA, rapid ruffling of the lamella was observed along the leading edge, including the lateral cell margins. In all cells this was followed by a rapid decrease in cell speed, that on average became reduced by $\sim 74\%$, $n=6$ (Figs 3A and 7B) followed by a $\sim 87\%$ increase in traction stress. This value is very similar to that which was seen after a calcium transient but occurred at a slower rate (Fig. 7B). In general there was no significant change in cell shape following EGTA treatment; however, in this example a slight elongation in shape occurred. One interesting feature of these results is the abrupt decrease in cell speed following EGTA treatment that occurred before any changes in cell shape, suggesting that cell movement can be inhibited before any detectable increase in traction stress. The rise in traction stress following EGTA treatment was also surprising since calcium transients are inhibited and decreased $[Ca^{2+}]_i$ is expected to reduce cytoskeletal contractility, as has been found in other systems (Sieck et al., 2001). This suggests that cytoskeletal tension can increase in a calcium/myosin II-independent manner and is supported by the finding that isolated stress fibers can contract in the absence of calcium, which involves Rho kinase activity (Katoh et al., 2001). The fact that retraction failed to occur, despite a comparable rise in traction stress to that which follows a calcium transient, is a strong indication that transients normally facilitate adhesion disassembly. Similar results were obtained when keratocytes were placed in Ca^{2+} -free medium ($n=6$, Fig. 7).

To further investigate the effect of EGTA treatment on adhesion turnover, cells were observed with IRM before and after treatment with 10 mM EGTA. In all cells ($n=10$) the region of close contact at the lateral rear edges became more prominent after ~ 30 seconds (Fig. 3C). When cell movement stopped ~ 1 minute after treatment, these regions had become darker and noticeably enlarged, consistent with a local increase in adhesion strength. Immunofluorescence studies of EGTA-treated keratocytes showed large accumulations of vinculin at the lateral cell edges, corresponding to locations where enlarged close contacts were seen by IRM (Fig. 4C,D). We conclude from this that the inhibition of calcium transients leads to a reduced rate of adhesion disassembly that results in a net increase in adhesion size and strength. A decreased rate of adhesion disassembly is expected to be particularly pronounced in regions where increased clustering of adhesion components has been shown to occur (Lee and Jacobson, 1997).

It was previously reported that an increase in the ratio of extracellular Mg^{2+}/Ca^{2+} can increase integrin-ligand binding affinity (Mould et al., 1995). Therefore, addition of EGTA may have a direct influence on adhesiveness in addition to its inhibitory effect on calcium transients. To abolish calcium transients without a directly affecting adhesiveness, keratocytes were treated with 100 μM gadolinium (Gd^{3+}), to block SACs. As with EGTA treatment, the first observable

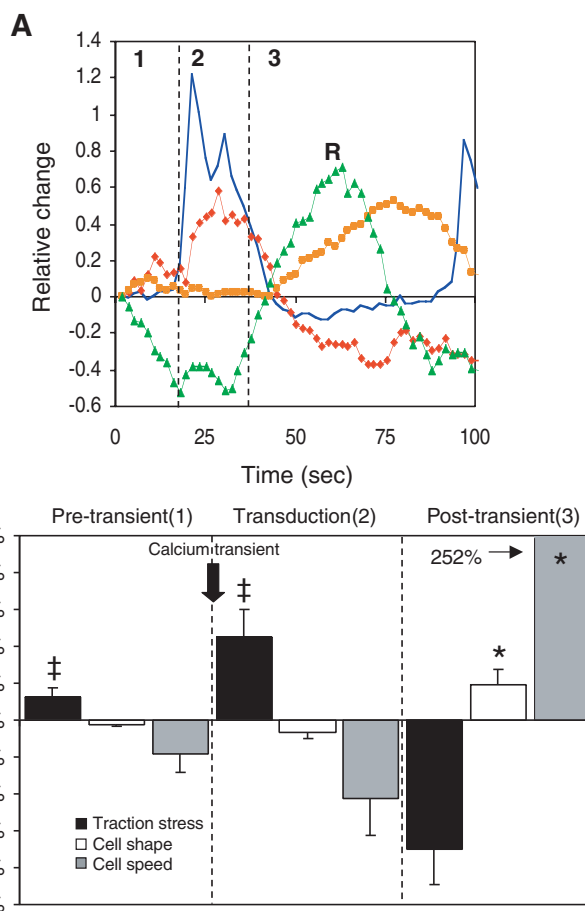
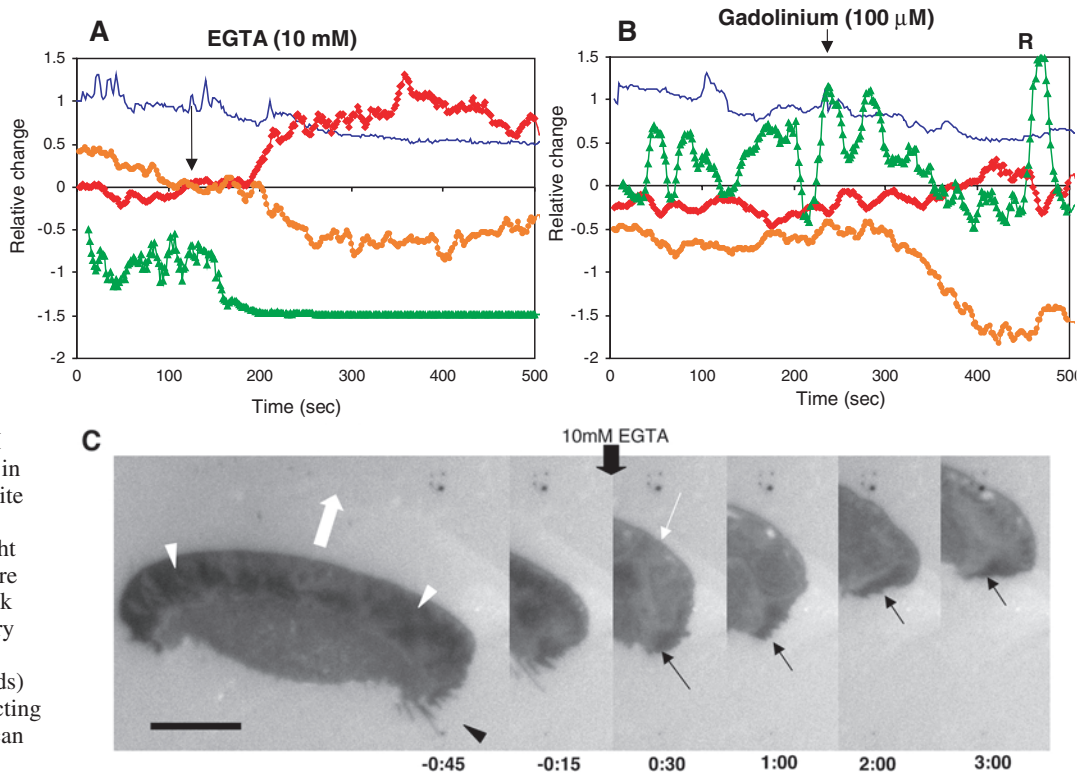


Fig. 2. The interrelationship between traction stress, cell shape and speed during one cycle of feedback. (A) An example of a single cycle of mechano-chemical feedback showing relative changes in traction stress (red), cell speed (green), shape factor (orange) and calcium indicator fluorescence (blue). Retraction of the rear cell margin is indicated (R). (B) The average relative changes in traction stress (black bar), cell speed (open bar) and shape (gray bar), associated with eight individual transients, for each phase of the feedback cycle. These are designated the pre-transient (1), transduction (2) and post-transient phases (3) and are also indicated in A. * indicates a significant difference ($P < 0.05$) from pre-transient and transduction measures. ‡ indicates a significant difference ($P < 0.05$) from measures of traction stress in all other phases.

effect was a ($\sim 68\%$) decrease in cell speed (Fig. 3B, Fig. 7A) that occurred between 0 and 60 seconds after addition of Gd^{3+} ($n=5$), but this occurred more slowly than following EGTA treatment (Fig. 7B). Meanwhile, traction increased slowly to an average value of ($\sim 36\%$) compared with EGTA treatment ($\sim 87\%$, Fig. 3A,B). In general, cell shape did not change significantly following Gd^{3+} treatment, although the degree of elongation was greater than after EGTA treatment. Overall, the effects of Gd^{3+} on mechano-chemical feedback were similar but less pronounced than following the addition of EGTA, possibly because adhesion disassembly is not fully inhibited. This is supported by finding that retraction and release of cytoskeletal tension can occur occasionally in the presence of Gd^{3+} (Fig. 3B), which explains why only a small average increase in traction stress is observed. Nevertheless, large accumulations of vinculin were seen at the lateral rear edges

Fig. 3. Inhibition of calcium transients prevents retraction and cell movement but not the generation of traction stress. (A,B) Plots of the relative changes in traction stress (red), cell speed (green), cell shape (orange) and calcium indicator fluorescence (blue). Each graph was offset for clarity and values for shape factor were multiplied by 3, for illustrative purposes. The addition of EGTA (A) or Gd^{3+} (B) is indicated (arrow), as is the retraction (R). (C) IRM images of an entire cell moving in the direction indicated (bold white arrow), and insets showing a retracting cell margin on the right side, at various time points before and after the addition (bold black arrow) of EGTA. Regions of very close contact beneath the lamellipodium (white arrowheads) and retraction fibers at the retracting rear margin (black arrowhead) can be seen before EGTA addition.

After treatment (bold black arrow) retraction fibers disappear, indicating a reduction in the rate of retraction. A region of very close contact at the rear cell margin begins to enlarge ~30 seconds later (arrow) and becomes more distinct after 2-3 minutes, by which time retraction is inhibited. Bar, 10 μ m.



of Gd^{3+} -treated keratocytes (Fig. 4E,F), suggesting that adhesion disassembly is inhibited in these regions. These data provide additional confirmation that SAC-mediated calcium transients normally increase the rate of adhesion disassembly at retracting cell margins.

Extracellular disruption of adhesions can induce retraction when calcium transients are inhibited

We have shown that when transients do not occur, retraction is prevented primarily because adhesion disassembly is inhibited, but not because of insufficient traction stress generation. To test this idea we treated keratocytes with 5 mM EDTA, a chelator of divalent cations (Mg^{2+} , Ca^{2+} , Mn^{2+}), which is known to disrupt adhesions and cause cell detachment. EDTA also leads to a reduction in $[Ca^{2+}]_i$ and inhibits calcium transients. In all cells examined ($n=9$), adding EDTA caused an immediate halt to cell movement (Fig. 5A) and a dramatic increase in lamellar ruffling. Retraction quickly followed but was much more extensive than following a calcium transient. It would usually start at one edge and continue along the entire cell margin (Fig. 5B). During retraction a large, ~62% drop in traction stress occurred, at a rate similar to that induced by a calcium transient, and was accompanied by a dramatic increase in cell roundness (Fig. 5A,B). Following EDTA induced retraction, cell movement did not resume, because cell polarity was abolished and cell spreading could not occur. These data indicate that retraction is limited by adhesion disassembly, especially when contractile force is insufficient to disrupt adhesions.

Calcimycin-induced calcium transients increase the rates of contractile force generation and adhesion disassembly

The fact that EDTA can induce retraction at the same rate as a calcium transient raises a question regarding the role of increased contractility in retraction. To address this question we treated cells with 5 μ M of the calcium ionophore, calcimycin (A-23187), which has previously been shown to induce a transient rise in $[Ca^{2+}]_i$ and retraction in keratocytes (Ishihara et al., 1997; Lee et al., 1999). We then compared the effects of this treatment with the changes in traction stress, cell speed and shape associated with a SAC-mediated calcium transient.

The addition of calcimycin resulted in an immediate increase in $[Ca^{2+}]_i$ that was maintained for ~1 minute. In all cells this induced an extensive retraction within ~30 seconds, which is somewhat faster than what we observed following a calcium transient. In addition, retractions were frequently more extensive, involving both lateral rear edges, and thus were associated with a greater increase in cell roundness (Fig. 6A,B). In half the cells examined, speed decreased while traction stress increased or was unchanged. This could be due to adhesion strengthening, since IRM observations showed a brief enlargement of close contacts at the retracting edge of a calcimycin-treated keratocyte (Fig. 6B). In the remaining group of cells, calcimycin treatment led to an immediate retraction, as shown by a rapid increase in cell speed and cell roundness. However, traction stress did not decrease as would be expected during retraction; instead this measure increased or was unchanged. A possible explanation for this observation

is that the rate of contractile force generation is sufficient to compensate for cell detachment, which would otherwise reduce traction stress. This is supported by finding that the average changes in traction force production and cell speed following calcimycin treatment occur more rapidly than following a calcium transient (Fig. 7B). We conclude from this that increased $[Ca^{2+}]_i$ can increase the rate of contractile force generation and adhesion disassembly.

Calcium-induced increases in contractility and adhesion disassembly act synergistically to increase cell speed

Previous observations of keratocytes moving on glass showed that transients occur more frequently in slow-moving, elongated cells (Lee et al., 1999). This was assumed to be partly due to increased cytoskeletal tension, and because the stronger adhesions in these cells required multiple transients for retraction. To investigate this possibility, and to determine the effect of frequent SAC-mediated calcium transients on cell speed, we compared cell speed with transient frequency. However, since cell adhesiveness is known to have a profound influence on cell speed, we needed to reduce the impact of this variable on our comparison. To do this, cells were sorted into two groups based on the standard deviation of the 90th percentile traction stress for the entire period of observation which provided a measure of average adhesiveness. Increased transient frequency in cells with low adhesiveness had no significant effect on cell speed or average 90th percentile traction stress (Fig. 8). However, in more adhesive cells, increased transient frequency was associated with a significant increase in speed, compared with cells displaying fewer transients, and cells of lower adhesiveness, regardless of transient frequency. This suggests that the detachment of weak adhesions is less dependent on increased adhesion disassembly than more adhesive cells. In other words, weaker adhesions are more dependent on force-induced retraction than on the disassembly of adhesions, which is in accordance with theoretical predictions (Di Milla et al., 1991). A comparison between cells of low and high adhesiveness, which both display frequent transients, showed that traction stress and speed were both significantly greater in more adhesive cells. This strongly supports the idea that calcium-induced increases in contractility and rate of adhesion disassembly act synergistically to promote rapid movement, especially as increased traction stress would normally be associated with a reduction in cell speed.

Discussion

We have investigated how calcium-induced changes in traction stress are correlated with cell speed and shape during the mechano-chemical feedback regulation of keratocyte movement. Cyclic changes in traction stress, cell speed and shape were associated with single calcium transients. In addition, an inverse relationship was found between traction stress and cell speed, suggesting that alternating changes in adhesiveness occur. Initially, adhesions are sufficiently strong to withstand the calcium-induced increase in contractility, whereas before retraction, adhesion weakening is attributed to both contractility and an increased rate of adhesion disassembly. Together, our data reveal a mechanism in which

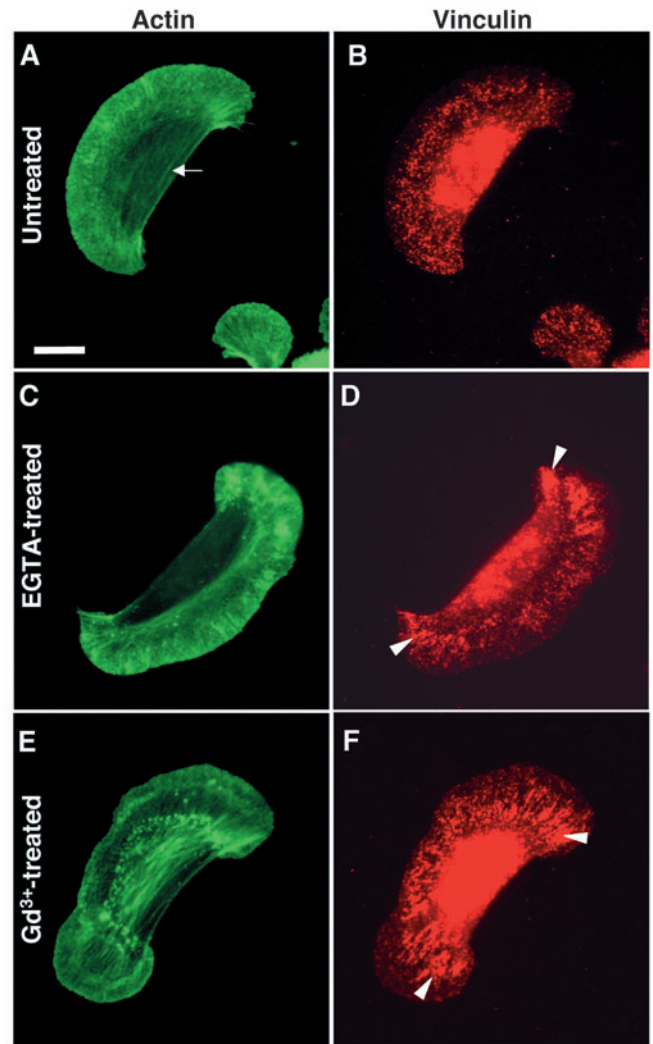


Fig. 4. Immunofluorescence staining of the actin cytoskeleton and vinculin in untreated keratocytes and cells treated with EGTA or gadolinium. Phalloidin staining of the actin cytoskeleton in untreated cells (A) and those treated with EGTA (C) or Gd^{3+} (E). Note in A the prominent centrally located stress fibers (white arrow). (B) Anti-vinculin antibody staining of untreated keratocytes showed a uniform distribution of vinculin puncta throughout the cell that increased in density a short distance behind the leading edge. Anti-vinculin antibody staining of keratocytes treated with EGTA (D) or Gd^{3+} (E) displayed large aggregations of vinculin within focal adhesion-like structures at the lateral rear cell margins (white arrowheads). The cell body appears brighter due to its increased thickness compared with the lamella. Bar, 10 μ m.

the regulation of adhesiveness by intracellular calcium is integrated into the SAC-mediated feedback regulation of keratocyte movement.

Cell elongation does not accompany increases in traction stress

The initiation of mechano-chemical signaling has been proposed to occur in response to increased cytoskeletal tension when retraction at the rear is impeded (Lee et al., 1999). Therefore, we were surprised to find that virtually no change

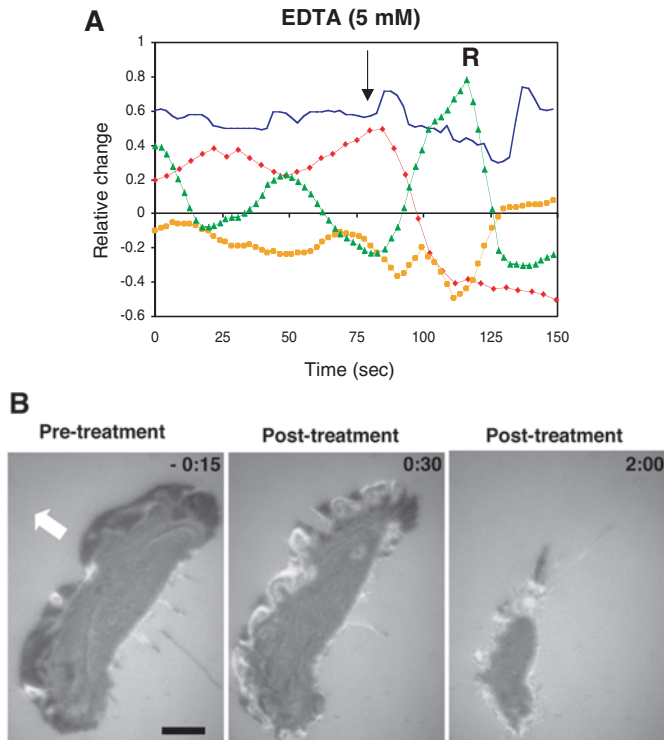


Fig. 5. Effects of inducing cell detachment by chelating external Ca^{2+} and Mg^{2+} with EDTA. (A) The relative changes in traction stress (red), cell speed (green), cell shape (orange) and calcium indicator fluorescence (blue). Each graph was offset for clarity, and values for shape factor were multiplied by 3, for illustrative purposes. The addition of EDTA (A) is indicated (arrow), as well as retraction of the rear (R). (B) IRM observations of keratocytes before and after treatment with EDTA. Bar, 10 μm . Addition of EDTA (A) leads to an immediate drop in traction stress, together with an increase in cell speed and shape factor, indicative of rapid cell detachment. IRM observations of a moving keratocyte in the direction indicated (bold white arrow) show cell detachment beginning at the leading edge 30 seconds after treatment, followed by retraction of the entire cell margin at 2 minutes.

in cell shape occurred before or following a calcium transient when the largest increase in traction stress usually occurred. These findings suggest that only a small or highly localized stretch stimulus may be required to activate SACs, and that subsequent increases in traction stress do not necessarily involve stretching or elongation of the entire cell. Instead, it is possible that this lack of shape change may be due to the ability of stress fibers to undergo isometric contraction (Katoh et al., 2001), and this is supported by the finding that keratocytes of similar size and shape produce traction stresses over a range of magnitudes (Doyle et al., 2004). In addition, the high degree of mechanical coupling between the cell front and rear could lead to an almost instantaneous halt to protrusion, if retraction is inhibited, and so might explain why increases in traction stress are not accompanied by cell elongation.

The inverse relationship between traction stress and cell speed arises from changes in cell adhesiveness
Cell adhesiveness has been described as arising from ‘grip’

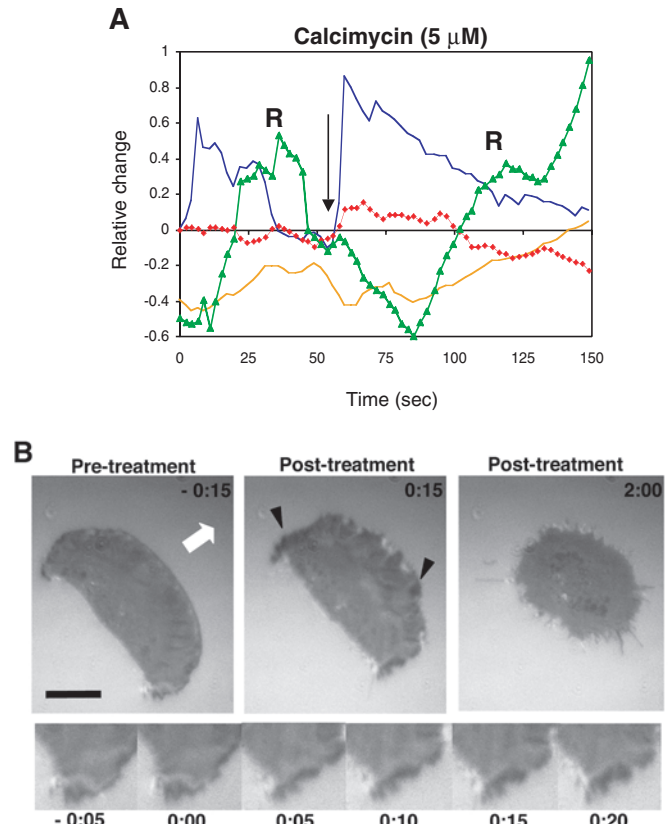


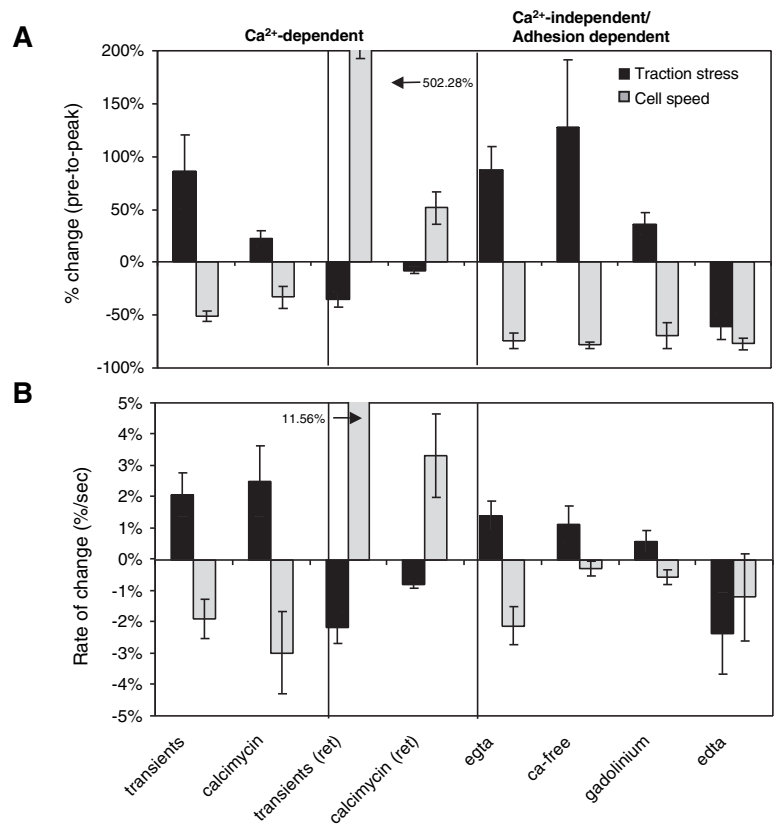
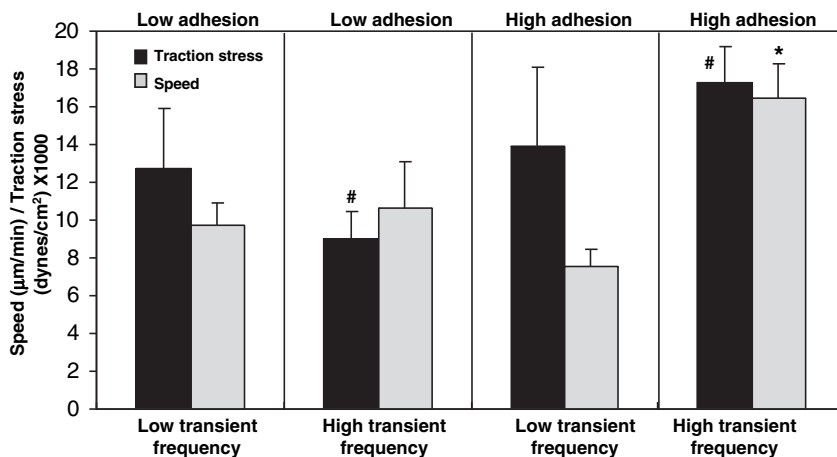
Fig. 6. Effects of inducing retraction by increasing $[\text{Ca}^{2+}]_i$ with calcimycin. (A) The relative changes in traction stress (red), cell speed (green), cell shape (orange) and calcium indicator fluorescence (blue). Each graph was offset for clarity, and values for shape factor were multiplied by 3, for illustrative purposes. The addition of calcimycin (A) is indicated (arrow), as well as retraction of the rear (R). The addition of calcimycin leads to a rapid increase in calcium indicator fluorescence, to a higher level and of longer duration than the SAC-mediated calcium transients. Traction stress increases slightly at 60 seconds while cell speed decreases. Retraction begins at ~80 seconds, as shown by the rapid increase in cell speed and slower cell rounding. (B) IRM observations of a treated keratocyte moving in the direction indicated (arrow) confirm that a brief period of adhesion strengthening occurs at the lateral rear and front edges (black arrowheads) between 0 and 20 seconds after calcimycin addition. The intervening time points are shown as insets. Note the increasing thickness of the line of very close contact, along the cell margin. In this example, retraction starts at the lateral cell edges and continues along the entire cell margin, until completed at 2 minutes.

and ‘stick’ (Rees et al., 1977), where grip corresponds to cytoskeletal contractility and stick refers to adhesion receptor-ligand binding affinity. According to this view, the large increase in traction stress and decreased cell speed that we observed during the transduction phase of the feedback cycle represents an increase in cell adhesiveness. However, without an independent measure of adhesion strength or ‘stickiness’, it is not possible to determine whether this contributes to the rise in traction stress. Nevertheless, it is possible that during the transduction phase, adhesions are already strong enough to support a calcium-induced increase in contractility, or adhesion strengthening occurs to sustain the rise in traction stress. Our observations support the latter, as by IRM, regions of close

Fig. 7. Summary histogram of relative magnitudes and rates of change in traction stress and cell speed under all experimental conditions and for different phases of the feedback cycle. (A) Percent change in traction stress (black) and cell speed (gray), before increases in $[Ca^{2+}]_i$ and after calcium-induced retractions, and treatments that inhibit calcium transients. (B) Rate of change (percent/second) of the parameters shown in A. In all cases an inverse relationship exists between traction stress and cell speed, except for EDTA treatment.

contact become larger and more prominent following a calcimycin-induced calcium transient. In addition, focal adhesion-like structures can form at the rear edges of moving keratocytes, where traction stress is highest (Lee and Jacobson, 1997). Furthermore, several mechanisms of force-dependent adhesion strengthening have been characterized, such as increased binding of adhesion proteins to actin filaments (Sawada and Sheetz, 2002), clustering of adhesion components (Wang et al., 1993; Plopper and Ingber, 1993), enlargement of adhesions (Balaban et al., 2001), strengthening of adhesion-cytoskeletal linkages (Choquet et al., 1997) or reinforcement of the actin cytoskeleton in these regions (Glogauer et al., 1997). The reduction in cell speed that we observe during this time is also consistent with an increase in adhesiveness, as an inverse relationship between cell speed and adhesiveness (when above optimum) has been shown (Palecek et al., 1997), and this has been indicated by previous comparisons between cell speed and traction force in other cell types (Harris et al., 1981; Oliver et al., 1994).

The advantage of strengthening adhesions following a calcium transient may be to increase their susceptibility to calcium-dependent disassembly mechanisms (Burrige and Chrzanowska-Wodnicka, 1996). Thus, cell detachment could be localized to regions under the greatest stress. This is consistent with our observation of a brief increase in the area of close contacts at the rear edges, immediately preceding retraction, when keratocytes are treated with calcimycin. However, when cell detachment is induced by treating keratocytes with EDTA, pre-strengthening of adhesions does not occur, resulting in retraction of the entire cell margin.



Calcium-induced increases in cytoskeletal contractility and adhesion disassembly facilitate retraction

The changes in traction stress and cell behavior that occur when calcium transients are either inhibited or induced have led us to conclude that both contractility and adhesion disassembly are involved in retraction. The accumulation of vinculin at retracting cell edges following EGTA or gadolinium treatment is a strong indication that retraction is dependent on calcium-induced adhesion disassembly. Inhibition of adhesion disassembly may contribute to an increase in adhesiveness at the rear, especially as traction stress can rise to similar levels observed after calcium transients, without inducing retraction. Evidence for this comes from the finding that $\beta 1$ integrins accumulate at the tail end of motile vascular smooth muscle cells and neutrophils, when calcium transients are inhibited by buffering of $[Ca^{2+}]_i$ (Pierini et al., 2000; Scherberich et al., 2000). The sudden increase in speed that we observe when a calcium transient induces retraction, or

Fig. 8. Summary histogram of the effects of calcium transient frequency on cell speed. In cells that are less adhesive transient frequency has no significant effect on the average 90th percentile traction stress (dark bar) or cell speed (stippled bar). By contrast, transient frequency is associated with a significant increase in average 90th percentile traction stress and cell speed in cells that are more adhesive. * indicates a significant difference ($P < 0.05$) from all other measures of cell speed. # indicates a significant difference ($P < 0.05$) between these two measures only.

following calcimycin treatment, is consistent with an increase in rate of adhesion disassembly, and is in accord with the prediction that a rapid retraction will typically occur when integrin-cytoskeletal linkages are cleaved (Palecek et al., 1999). An increase in contractility is also implicated in calcimycin-induced retractions because a rise in traction stress can occur just before the rear edge detaches. Calcium-induced increases in contractility and adhesion disassembly also appear to act synergistically to induce retraction. This could explain why the fastest moving keratocytes display the highest frequency of calcium transients and generate the largest average 90th percentile traction stress.

We conclude that the regulation of cell adhesiveness by SAC-induced calcium transients drives repeated cycles of protrusion and retraction. In addition, the differential response of adhesions at the front and rear to calcium transients may promote respective adhesion formation and disassembly, in these regions. Thus, older adhesions at the rear of keratocytes that experience longer periods of increased stress (Doyle et al., 2004) may be more likely to disassemble in response to increased $[Ca^{2+}]_i$, while newer adhesions may be strengthened by increased contractility and by elevated $[Ca^{2+}]_i$ (Pelletier et al., 1992; Rowin et al., 1998). Such coordination between mechano-sensing at adhesions and the activation of SACs provides a basis for understanding how cytoskeletal function is organized spatially and temporally to drive cell movement.

This work was supported by a National Science Foundation Grant MCB-0114231 to J.L.

References

- Balaban, N. Q., Schwarz, U. S., Riveline, D., Goichberg, P., Tzur, G., Sabanay, I., Mahalu, D., Safran, S., Bershadsky, A., Addadi, L. et al. (2001). Force and focal adhesion assembly: a close relationship studied using elastic micropatterned substrates. *Nat. Cell Biol.* **3**, 466-472.
- Brundage, R. A., Fogarty, K. E., Tuft, R. A. and Fay, F. S. (1991). Calcium gradients underlying polarization and chemotaxis of eosinophils. *Science* **254**, 703-706.
- Brust-Mascher, I. and Webb, W. W. (1998). Calcium waves induced by large voltage pulses in fish keratocytes. *Biophys. J.* **75**, 1669-1678.
- Burridge, K. and Chrzanowska-Wodnicka, M. (1996). Focal adhesions, contractility, and signaling. *Annu. Rev. Cell Dev. Biol.* **12**, 463-518.
- Burton, K., Park, J. H. and Taylor, D. L. (1999). Keratocytes generate traction forces in two phases. *Mol. Biol. Cell* **10**, 3745-3769.
- Chen, W.-T. (1979). Induction of spreading during fibroblast movement. *J. Cell Biol.* **81**, 684-691.
- Chen, W.-T. (1981). Mechanism of retraction of the trailing edge during fibroblast movement. *J. Cell Biol.* **90**, 159-187.
- Choquet, D., Felsenfeld, D. P. and Sheetz, M. P. (1997). Extracellular matrix rigidity causes strengthening of integrin-cytoskeleton linkages. *Cell* **88**, 39-48.
- Crowley, E. and Horwitz, A. F. (1995). Tyrosine phosphorylation and cytoskeletal tension regulate the release of fibroblast adhesions. *J. Cell Biol.* **131**, 525-537.
- Dembo, M. and Wang, Y.-L. (1999). Stresses at the cell-to-substrate interface during locomotion of fibroblasts. *Biophys. J.* **76**, 2307-2316.
- DiMilla, P. A., Barbee, K. and Lauffenburger, D. A. (1991). Mathematical model for the effects of adhesion and mechanics on cell migration speed. *Biophys. J.* **60**, 15-37.
- Doyle, A. D. and Lee, J. (2002). Simultaneous, real-time imaging of intracellular calcium and cellular traction force production. *Biotechniques* **33**, 358-364.
- Doyle, A., Marganski, B. and Lee, J. (2004). Calcium transients induce spatially coordinated increases in traction force during the movement of fish keratocytes. *J. Cell Sci.* **117**, 2203-2214.
- Eddy, R., Pierini, L. M., Matsumura, F. and Maxfield, F. R. (2000). Ca^{2+} -dependent myosin II activation is required for uropod retraction during neutrophil migration. *J. Cell Sci.* **113**, 1287-1298.
- Galbraith, C. G. and Sheetz, M. P. (1997). A micromachined device provides a new bend on fibroblast traction forces. *Proc. Natl. Acad. Sci. USA* **94**, 9114-9118.
- Giannone, G., Ronde, P., Gaire, M., Haich, J. and Takeda, K. (2002). Calcium oscillations trigger focal adhesion disassembly in human U87 astrocytoma cells. *J. Biol. Chem.* **277**, 26364-26371.
- Gilbert, S. H., Perry, K. and Fay, F. S. (1994). Mediation of chemoattractant-induced changes in $[Ca^{2+}]_i$ and cell shape, polarity and locomotion by InsP₃, DAG, and protein kinase C in newt eosinophils. *J. Cell Biol.* **127**, 489-503.
- Glogauer, M., Arora, P., Yao, G., Sokholov, I., Ferrier, J. and McCulloch, C. A. G. (1997). Calcium ions and tyrosine phosphorylation interact coordinately with actin to regulate cytoprotective responses to stretching. *J. Cell Sci.* **110**, 11-21.
- Gomez, T. M., Robles, E., Poo, M. and Spitzer, N. C. (2001). Filopodial calcium transients promote substrate-dependent growth cone turning. *Science* **291**, 1983-1987.
- Harris, A. K. (1980). Silicone rubber substrata: a new wrinkle in the study of cell locomotion. *Science* **208**, 177-179.
- Harris, A. K., Stopak, D. and Wild, P. (1981). Fibroblast traction as a mechanism for collagen morphogenesis. *Nature* **290**, 249-251.
- Hartwig, J. H. and Yin, H. (1988). The organization and regulation of the macrophage cytoskeleton. *Cell Motil. Cytoskeleton* **10**, 117-125.
- Hendey, B., Klee, C. B. and Maxfield, F. R. (1992). Inhibition of neutrophil chemokinesis on vitronectin by inhibitors of calcineurin. *Science* **258**, 296-299.
- Huttenlocher, A., Palecek, S. P., Lu, Q., Zhang, W., Mellgren, R. L., Lauffenburger, D. A., Ginsberg, M. H. and Horwitz, A. F. (1997). Regulation of cell migration by the calcium-dependent protease calpain. *J. Biol. Chem.* **272**, 32719-32722.
- Ishihara, A., Gee, K., Schwartz, S., Jacobson, K. and Lee, J. (1997). Photoactivation of caged compounds in single, living cells: an application to the study of cell locomotion. *Biotechniques* **23**, 268-274.
- Katoh, K., Kaibuchi, Y. and Fujiwara, K. (2001). Rho-kinase-mediated contraction of isolated stress fibers. *J. Cell Biol.* **153**, 569-583.
- Kolega, J. (1986). Effects of mechanical tension on protrusive activity and microfilament and intermediate filament organization in an epidermal epithelium moving in culture. *J. Cell Biol.* **102**, 1400-1411.
- Lauffenburger, D. A. and Horwitz, A. F. (1996). Cell migration: a physically integrated molecular process. *Cell* **84**, 359-369.
- Leader, W. M., Stopak, D. and Harris, A. K. (1983). Increased contractile strength and tightened adhesions to the substratum result from reverse transformation of CHO cells by dibutyl cyclic adenosine monophosphate. *J. Cell Sci.* **64**, 1-11.
- Lee, J. and Jacobson, K. (1997). The composition and dynamics of cell-substratum adhesions in locomoting fish keratocytes. *J. Cell Sci.* **110**, 2833-2844.
- Lee, J., Ishihara, A., Theriot, J. and Jacobson, K. (1993). Principles of locomotion for simple-shaped cells. *Nature* **362**, 167-171.
- Lee, J., Leonard, M., Oliver, T., Ishihara, A. and Jacobson, K. (1994). Traction forces generated by locomoting keratocytes. *J. Cell Biol.* **127**, 1957-1964.
- Lee, J., Ishihara, A., Oxford, G., Johnson, B. and Jacobson, K. (1999). Regulation of cell movement is mediated by stretch-activated calcium channels. *Nature* **400**, 382-386.
- Lo, C.-M., Wang, H.-B., Dembo, M. and Wang, Y.-L. (2000). Cell movement is guided by the rigidity of the substrate. *Biophys. J.* **79**, 144-152.
- Mandeville, J. T., Ghosh, R. N. and Maxfield, F. R. (1995). Intracellular calcium levels correlate with speed and persistent forward motion in migrating neutrophils. *Biophys. J.* **68**, 1207-1217.
- Marganski, W. A., Dembo, M. and Wang, Y.-L. (2003). Measurements of cell-generated deformations on flexible substrata using correlation-based optical flow. *Methods Enzymol.* **161**, 197-211.
- Marks, P. W. and Maxfield, F. R. (1990). Transient increases in cytosolic free calcium appear to be required for the migration of adherent human neutrophils. *J. Cell Biol.* **110**, 43-52.
- Mitchison, T. J. and Cramer, L. P. (1996). Actin-based cell motility and cell locomotion. *Cell* **84**, 371-379.
- Mould, A. P., Akiyama, S. K. and Humphries, M. J. (1995). Regulation of integrin alpha 5 beta 1-fibronectin interactions by divalent cations. Evidence for distinct classes of binding sites for Mn^{2+} , Mg^{2+} , and Ca^{2+} . *J. Biol. Chem.* **270**, 26270-26277.
- Nebl, T. and Fisher, P. R. (1997). Intracellular Ca^{2+} signals in Dictyostelium

- chemotaxis are mediated exclusively by Ca^{2+} influx. *J. Cell Sci.* **110**, 2845-2853.
- Oliver, T., Lee, J. and Jacobson, K.** (1994). Forces exerted by locomoting cells. *Semin. Cell Biol.* **5**, 139-147.
- Oliver, T., Dembo, M. and Jacobson, K.** (1999). Separation of propulsive and adhesive traction stresses in locomoting keratocytes. *J. Cell Biol.* **145**, 589-604.
- Palecek, S. P., Loftus, J. C., Ginsberg, M. H., Lauffenberger, D. A. and Horwitz, A. F.** (1997). Integrin-ligand binding properties govern cell migration speed through cell-substratum adhesiveness. *Nature* **385**, 537-540.
- Palecek, S., Horwitz, A. and Lauffenberger, D.** (1999). Kinetic model for integrin-mediated adhesion release during cell migration. *Ann. Biomed. Eng.* **27**, 219-235.
- Pelham, R. J. and Wang, Y.-L.** (1999). High resolution detection of mechanical forces exerted by fibroblasts on the substrate. *Mol. Biol. Cell* **10**, 935-945.
- Pelletier, A. J., Bodary, S. C. and Levinson, A. D.** (1992). Signal transduction by the platelet integrin alpha IIb beta 3, induction of calcium oscillations required for protein-tyrosine phosphorylation and ligand-induced spreading of stably transfected cells. *Mol. Biol. Cell* **3**, 989-998.
- Pierini, L. M., Lawson, M. A., Eddy, R. J., Hendey, B. and Maxfield, F. R.** (2000). Oriented endocytic recycling of alpha5beta1 in motile neutrophils. *Blood* **95**, 2471-2480.
- Plopper, G. and Ingber, D. E.** (1993). Rapid induction and isolation of focal adhesion complexes. *Biochem. Biophys. Res. Commun.* **193**, 571-578.
- Pollard, T. D. and Borisy, G. G.** (2003). Cellular motility driven by assembly and disassembly of actin filaments. *Cell* **112**, 453-465.
- Rees, D. A., Lloyd, C. W. and Thom, D.** (1977). Control of grip and stick in cell adhesion through lateral relationships between of membrane glycoproteins. *Nature* **267**, 124-128.
- Robles, E., Huttenlocher, A. and Gomez, T. M.** (2003). Filopodial calcium transients regulate growth cone motility and guidance through local activation of calpain. *Neuron* **38**, 597-609.
- Rowin, M. E., Whatley, R. E., Yednock, T. and Bohnsack, J. F.** (1998). Intracellular calcium requirements for beta1 integrin activation. *J. Cell Physiol.* **175**, 193-202.
- Sawada, Y. and Sheetz, M. P.** (2002). Force transduction by triton cytoskeletons. *J. Cell Biol.* **156**, 609-15.
- Scherberich, A., Campos-Toimil, M., Ronde, P., Takeda, K. and Beretz, A.** (2000). Migration of human vascular smooth muscle cells involves serum-dependent repeated cytosolic calcium transients. *J. Cell Sci.* **113**, 653-662.
- Schmidt, C. E., Horwitz, A. F., Lauffenberger, D. A. and Sheetz, M. P.** (1993). Integrin-cytoskeletal interactions in migrating fibroblasts are dynamic asymmetric and regulated. *J. Cell Biol.* **123**, 977-991.
- Sieck, G. C., Han, Y.-S., Pabelick, C. M. and Prakask, Y. S.** (2001). Temporal aspects of excitation-contraction coupling in airway smooth muscle. *J. Appl. Physiol.* **91**, 266-274.
- Sjaastad, M. D. and Nelson, J.** (1996). Integrin-mediated calcium signaling and regulation of cell adhesion by intracellular calcium. *Bioessays* **19**, 47-55.
- Stossel, T. P.** (1993). On the crawling of animal cells. *Science* **260**, 1086-1094.
- Walker, J. W., Gilbert, S. H., Drummond, R. M., Yamada, M., Sreekumar, R., Carraway, R. E., Ikeebe, M. and Fay, F.** (1998). Signaling pathways underlying eosinophil cell motility revealed by using caged peptides. *Proc. Natl. Acad. Sci. USA* **95**, 1568-1573.
- Wang, N., Butler, J. P. and Ingber, D. E.** (1993). Mechanotransduction across the cell surface and through the cytoskeleton. *Science* **260**, 1124-1127.
- Zeng, Q., Lagunoff, D., Masaracchia, R., Goeckeler, Z. and Cote, G.** (2000). Endothelial cell retraction is induced by PAK2 monophosphorylation of myosin II. *J. Cell Sci.* **113**, 471-482.